COMPARISON OF NANOCRYSTALS FROM TEMPO OXIDATION OF BAMBOO, SOFTWOOD, AND COTTON LINTER FIBERS WITH ULTRASONIC-ASSISTED PROCESS

Yun Qian, Zhongyan Qin, Ngoc-Minh Vu, Guolin Tong,* and Y. C. Frank Chin

Fully bleached kraft bamboo pulp (BPFs), fully bleached kraft softwood pulp (SPFs), and bleached cotton linter pulp (CPFs), which have different crystallinities, were oxidized in the TEMPO-NaBr-NaClO system with ultrasonic treatment for producing nanocrystals. The carboxylate content of nanocrystals made from BPFs, SPFs, and CPFs were 2.10, 2.02, and 1.66 mmol/g, respectively. Nanocrystals of BPFs and SPFs had widths of 5 to 15 nm and lengths of 400 to 800 nm. The length and width of CPFs nanocrystals were 200 to 400 nm and 15 to 25 nm. The oxidizing rates of BPFs, SPFs, and CPFs were different. These differences could be attributed to crystallinity. Crystallinity affected microstructures, chemical process, and the efficiency of ultrasonication. Crystallinity also shaped the nanocrystals, since nanocrystals consist of the residual crystalline regions after chemical oxidation and ultrasonication. Fibers of lower crystallinity (such as bamboo) showed a higher reactivity, and the nanocrystals made from low crystallinity materials were longer, thinner, more rapidly formed, and required less energy in their preparation.

Keywords: Cotton linter fibers; Bamboo fibers; Softwood fibers; TEMPO oxidation; Crystallinity; Ultrasonic treatment; Nanocrystals

*Contact information: Jiangsu Provincial Key Lab of Pulp and Paper Science and Technology, Nanjing Forestry University, Nanjing 210037, China; *Corresponding author: gtong@njfu.edu.cn*

INTRODUCTION

Interest in nano-scale materials stems from the fact that new and outstanding properties may be acquired when the length scales of materials are greatly reduced, and those properties provide many potential applications (Samir *et al.* 2005; Wegner and Jones 2006). Cellulose fibers have long been used in various fields and many new applications have been explored (Eichhorn *et al.* 2010; Klemm *et al.* 2005). Cellulose fibers are advantageous in the production of nano-scale particles and bio-composites because the fibers are made from natural nano-scale components (Hubbe *et al.* 2008). Moreover, cellulose fibers are cheap, environmentally friendly, and are easily found from plant fibers. For these reasons, natural cellulose fibers are especially suitable to prepare nano-composites (Huber *et al.* 2012). Nanofibers and/or nanocrystals have been extracted from plants by many scientists and researchers (Bolio-Lopez *et al.* 2011; Cherian *et al.* 2011; Martins *et al.* 2011; Saito *et al.* 2007; Stelte and Sanadi 2009).

There are many methods to obtain nanofibers and/or nanocrystals from natural materials, but the major approaches to prepare cellulose nanofibers and/or nanocrystals involve mechanical treatment, enzymatic treatment, and/or chemical modification. However, it is not easy to obtain nanofibers and/or nanocrystals, since the cellulose structure is stable, and chemical reagents are blocked from reacting with active groups of fibers.

Mechanical treatments such as ultrasonication (Chen *et al.* 2011a,b), grinding (Abe and Yano 2009), and high-pressure homogenizer (Kaushik and Singh 2011) have been utilized to facilitate the chemical process. Ultrasonication generates ultrasonic cavitation in the solution and causes micro-bubbles. When micro-bubbles collapse, high energy is released and converted to high pressure and high temperature. The process causes degradation of polymers and/or catalytic acceleration of reactions (Kawasaki *et al.* 2007). Nanofibers have been obtained by simple ultrasonic treatment (Chen *et al.* 2011b), but nanofibers formed in this manner have been found to easily aggregate, and the method consumes a lot of energy. Nanocrystals are also obtained by acid hydrolysis assisted with ultrasonication (Filson and Dawson-Andoh 2009; Mishra *et al.* 2011).

There is a new method to obtain nanocrystals directly from cotton linter fibers by TEMPO-mediated oxidation assisted by ultrasonic treatment (Qin *et al.* 2011b). Because of its selectivity, TEMPO (2,2,6,6-tetramethyl-piperidine-N-oxyl) mediated oxidation is widely used in making nanofibers or nanocrystals. The nanocrystals obtained by TEMPO oxidation with ultrasonic treatment have high carboxylate content and thus tend to remain stably dispersed in water. Compared with simple chemical treatment and/or simple mechanical treatment, this method is faster and more convenient to operate, since it does not need post treatment and the products have functional groups (Qin *et al.* 2011a,b).

However, among those papers, factors affecting the process of producing nanofibers have rarely been considered (Saito and Isogai 2004). This paper will focus on the relationship between fiber crystallinities and their nano-products. The cotton linter pulp, softwood pulp, and bamboo pulp were selected as raw materials due to their different degrees of crystallinity and contrasting microstructures. Cotton linter is a kind of cellulose that has high crystallinity; morphological studies have shown that there were no significant differences among nanostructures from different kinds of cotton linter fibers, as well as no significant differences in shape and size (Teixeira *et al.* 2010). The crystallinity of softwood fibers is lower than that of cotton linter, but higher than bamboo fibers. Bamboo is one of the fastest growing grass-plants and is abundantly available in many countries (Lipp-Symonowicz *et al.* 2011). Each bamboo fiber contains many fibrils, and each of these fibrils contains abundant continuous elongated cellulose elements, which are staggered in the form of twisted wires (Ray *et al.* 2004). However, there are some impurities such as hemicellulose and little residual lignin in the pulp. In addition, bamboo pulp also contains parenchyma cells (Abe and Yano 2010).

EXPERIMENTAL

Materials

Fully bleached kraft bamboo pulp (from Guizhou Chitianhua, China), softwood pulp (from Howe Sound Pulp & Paper Corporation, Canada), and cotton linter pulp (from Anhui Xuelong Pulp Mill, China) were used as native cellulose fibers.

2,2,6,6-tetramethyl-piperidine-1-oxyl free radical (TEMPO, Changzhou JiaNa Chemical Co. Ltd., China), sodium bromide (Sinopharm Chemical Regent Co. Ltd., China), sodium hypochlorite solution (49 g/L available chlorine, Shanghai Jiuyi Chemical Co. Ltd., China), and other chemicals were all used as received without further purification.

An ultrasonic cleaner (KQ-300DE, Kunshan Ultrasound Instrument Co. Ltd., China) was used as an ultrasonic generator with working frequency of 40 kHz and ultrasonic power of 300 W. Its volume was 10 L.

TEMPO Oxidation with Ultrasonic Treatment

Fully bleached bamboo pulp fibers (BPFs), fully bleached softwood pulp fibers (SPFs), and cotton linter pulp fibers (CPFs) were dispersed in water (1 g dry fibers dispersed in 100 mL water), respectively. Sodium bromide (0.16 g, 1.6 mmol), TEMPO (0.016 g, 0.1 mmol), and sodium hypochlorite solution (29 mL, approximately 20 mmol) were added to each mixture. Then, the pH was adjusted to 10 by addition of 0.5 M hydrochloric acid. Each mixture was transferred to a four-neck flask. The flask was then dipped into the bath of the ultrasonic cleaner with a certain amount of distilled water. The ultrasonic cleaner was turned on and the power was set at 100%. The temperature of the mixture in the flask was maintained at 25 ^{o}C by circulating cooling water. The pH of the mixture was maintained at 10 by adding 0.5 M sodium hydroxide solution. At the end of oxidation, the solution was acidified until the pH was 2 to 3 by adding 0.5 M hydrochloric acid. The mixture was separated by centrifugation at 10,000 rpm for 10 mins. The precipitate was washed by water and centrifuged three times. The precipitate was then freeze-dried to obtain solid samples. The same treatments were done for BPFs, SPFs, and CPFs.

Scanning Electron Microscopy (SEM) of Fibers and Oxidized Fibers

The original and the oxidized BPFs, SPFs, and CPFs were observed with an ESEM (Quanta 200 environmental scanning electron microscopy FEI, Netherlands). It was operated at 20 kV, and the current changed with the vacuum of the observed circumstance.

Determination of Available Chlorine Content of Oxidation

The content of sodium hypochlorite was expressed in available chlorine, and the content of available chlorine was determined by the iodometric method (Shi and He 2010).

Determination of Carboxyl Content of Oxidized Cellulose Fibers

The carboxyl content of the untreated and the oxidized cellulose fibers was determined by the electrical conductivity titration method. A sample (0.1 g) was dispersed in 100 mL 0.001 M sodium chloride solution, and 0.1 mL 2 M hydrochloric acid was added to the sample. Then, the mixture was titrated with 0.05 M sodium hydroxide under a blanket of nitrogen in the presence of magnetic stirring. A conductance electrode was used to observe and record the changing process of conductivity. The total content of the oxidized fibers was calculated by the equation given by Qin *et al.* (2011b).

Crystallinity and Crystal Size Determination by X-Ray Diffraction (XRD)

The crystallinities of freeze-dried samples were determined by an X-ray diffractometer (DX-2000 Dandong Fangyuan Instrument Co. LTD., China). X-ray diffraction patterns were recorded from 10^{o} to 40^{o} of diffraction angle 2θ, λ = 0.154 nm.

Crystal size of cellulose I structure was calculated by Scherrer's equation,

$$D = 0.89\lambda / (\beta_{1/2} \cos\theta) \quad (1)$$

where θ is the diffraction angle, λ is the wavelength of the X-ray radiation, and $\beta_{1/2}$ is the full width at half heights of the diffraction peaks.

Crystallinity was determined by the equation,

$$\text{Relative crystallinity} = (I_{\text{crystalline}} - I_{\text{amorphous}}) \times 100\% / I_{\text{crystalline}} \quad (2)$$

where $I_{\text{crystalline}}$ is identified with the intensity at 22.5^{o}, and $I_{\text{amorphous}}$ is the intensity at 18.6^{o}.

Transmission Electron Microscopy (TEM) of Cellulose Nanocrystals

The nanocrystals were examined by transmission electron microscopy (HITACHI H7650, Japan). Suspension of oxidized fibers was diluted and dropped onto a copper grid. The copper grid was left to stand for drying. The dry sample was observed by TEM. The observation was operated at 80 kV.

RESULTS AND DISCUSSION

TEMPO Oxidation of BPFs, SPFs, and CPFs in Ultrasonic System

SEM observation of fibers of BPFs, SPFs, and CPFs during oxidation process

The fibrillation process during the reaction was investigated by sampling action. The samples, which were oxidized at different oxidation times during TEMPO oxidation in the ultrasonic system, were prepared and observed by SEM, and images are shown in Fig. 1.

As shown in Fig. 1(a), the surfaces of original CPFs were smooth, while those of BPFs and SPFs were full of pits and caves. SPFs were thicker than BPFs. These three fibers were changed dramatically during the oxidation. After a 1 h oxidation in the ultrasonic system (shown in (b)), all fibers were changed, but to different degrees: the peeling of the primary wall and secondary walls (S1) was obvious, and separated layers were generated from SPFs and BPFs; the primary wall and secondary wall (S1) were partly broken, and some pits and plaques were observed in CPFs. After two hours of oxidation (shown in (c)), the pits were deeper, and fine particles were found to be torn off the surface from all three fibers. The S2 wall was broken, and the lumen could be seen in BPFs and SPFs. The CPFs' microstructure was packed closely and hard to damage, so some of the S1 wall could still be seen. Furthermore, BPFs had more surface area than SPFs, and the CPFs had the least cracks and surface area. After three hours of oxidation (shown in (d)), all fibers were damaged severely: for cotton linter fibers, many microfibrils from the S2 wall began to be exposed to reagents; for softwood pulp fibers and bamboo pulp fibers, the lengths were shorter, and many fragments were found.

C6 primary hydroxyl groups are selectively oxidized to carboxyl groups by the TEMPO system; this reaction occurs on the surface (Montanari *et al.* 2005). Fibers become more and more hydrophilic when their hydroxyl groups are transformed to carboxyl groups gradually, and the process for fibrils to be separated and liberated became easier. Moreover, ultrasonic treatment helped liberate fibrils. Thus, from SEM images (a) to (d), fibers were smaller and thinner, and more fibrils were found. After oxidizing for 4 hrs, fragments of fibers could hardly be observed.

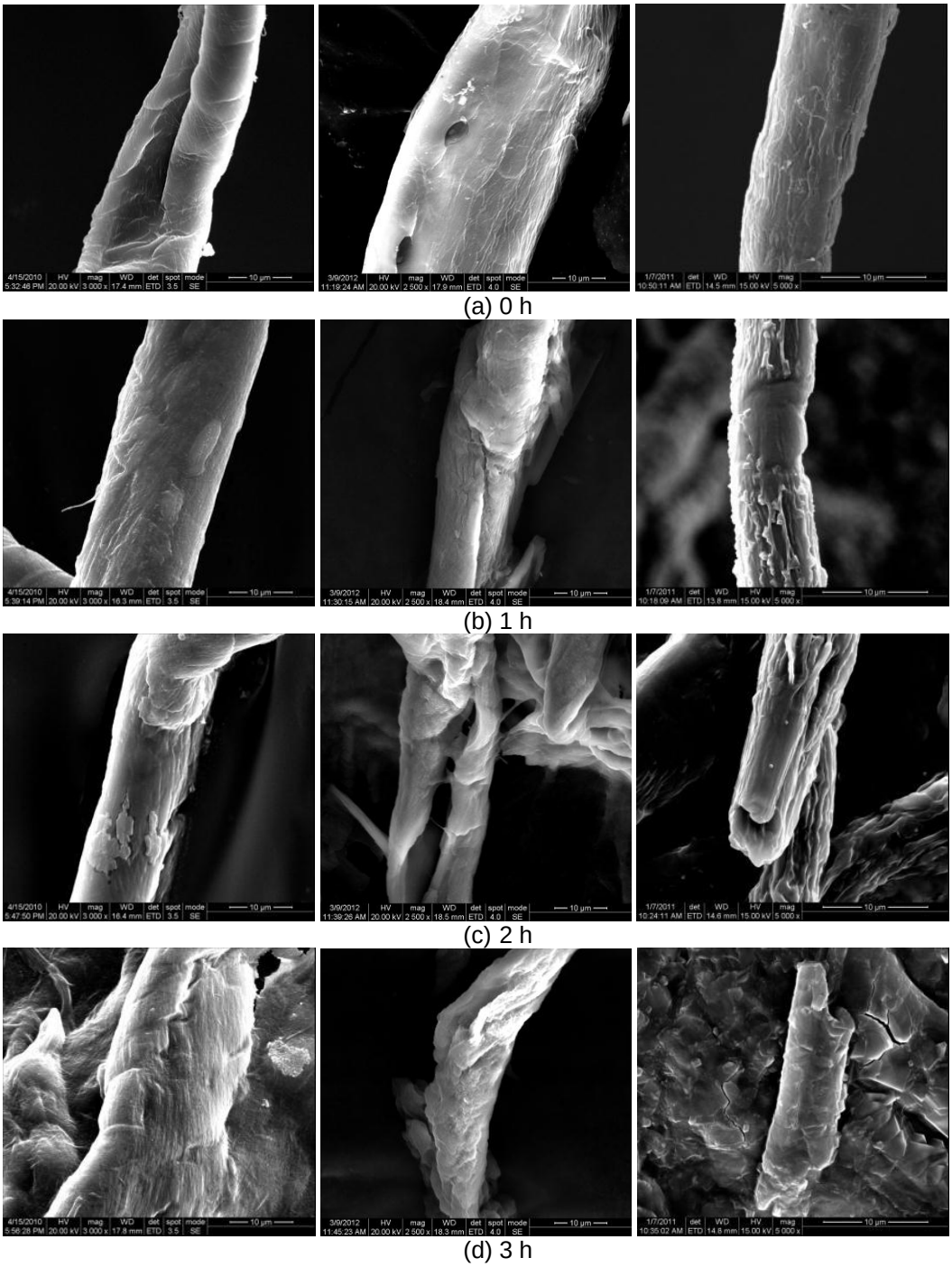

Fig. 1. SEM Images of CPFs, SPFs, and BPFs cellulose fibrils (from left to right) with different reaction times under the condition of the TEMPO oxidation in ultrasonic system (a) 0 h, (b) 1 h, (c) 2 h, (d) 3 h

The fibrillation process was greatly affected by the microstructures of fibers (Stelte and Sanadi 2009). Though ultrasonication is a strong treatment and could break the structure of fibers, the damage degrees of different kinds of fibers varied since the microstructures were different. For fibers having a high crystalline structure such as CPFs, the ultrasonication was less effective, and the fibrillation process needed more time. As a result, varying degrees of fibrillation will affect the chemical process and final products.

Change of Crystallinity of Cellulose during TEMPO Oxidation

As shown in Fig. 2 and Table 1, crystallinities of BPFs, SPFs, and CPFs increased before and after TEMPO oxidation with ultrasonic treatment. The crystallinity of BPFs increased the most, followed by that of SPFs. The crystallinity of CPFs increased the least.

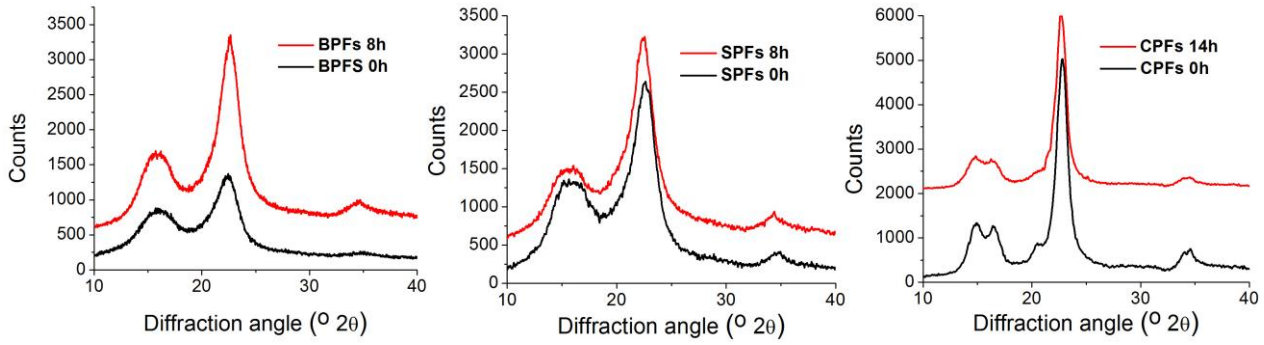

Fig. 2. X-ray diffraction patterns of the BPFs, SPFs, and CPFs. (A) BPFs: original BPFs (A0), and oxidized BPFs by TEMPO oxidation with ultrasonic system for 8 h (A1); (B) SPFs: original SPFs (B0), and oxidized SPFs by TEMPO oxidation with ultrasonic system for 8 h (B1); (C) CPFs: original CPFs (C0), and oxidized CPFs by TEMPO oxidation with ultrasonic system for 14 h (C1).

Table 1. Crystallinities and Crystal Sizes of BPFs, SPFs, and CPFs

Sample	Crystallinity (%)			Crystal Size (nm)		
	BPFs	SPFs	CPFs	BPFs	SPFs	CPFs
Original	66.1	72.3	83.7	3.1	2.9	7.0
After Oxidation	79.5	83.5	84.1	3.0	2.8	6.2

Table 1 shows the crystallinities and crystal sizes of original materials and their oxidized products. As previously cited, the BPF crystallinity was the lowest, SPF crystallinity was the second lowest, and CPF crystallinity was the highest. In the ultrasonic system, the micro-jets that were generated damaged the surface of the cellulose, thus accelerating the oxidation (Qin *et al.* 2011b). At the same time, the process of degradation would also be accelerated, as well as the hydrolyzation of amorphous region. Besides, the microfibril structure is capable of becoming delaminated when it is under ultrasonic conditions (Li and Renneckar 2009, 2011). So the amorphous region and the surface of crystalline region would be destroyed, and the crystallinity would increase. As BPFs' crystallinity was the lowest and there was more surface area, the oxidation was the fastest. It was also easier for the micro-jet to damage the structure of cellulose, since there was more amorphous region and surface. For CPFs, however, the high crystallinity and compact microstructure made ultrasonic treatment and oxidation less effective, so the crystallinity changed little. Since the crystallinity of SPFs was just between the

crystallinity of BPFs and CPFs, the crystallinity increased more than CPFs but less than BPFs.

The crystal sizes are also calculated, and results are shown in Table. 1. The crystal size of CPF was the biggest, and the crystallinity was the highest, so the surface oxidation on crystalline regions took a large proportion in the reaction. After the oxidation, the crystal size declined to 6.2 nm, which attributed to the oxidation of crystal size (Li and Renneckar 2011; Okita *et al.* 2010). The crystal size of BPF was 3.1 nm, and the crystal size of SPF was 2.9 nm, while the crystallinity of BPFs was higher than that of SPFs. The phenomenon indicated that the BPFs had more amorphous region than SPFs, which was located between two crystalline regions.

Consumption of available chlorine during reaction

The residual available chlorine was determined by the iodometric method, and results are shown in Fig. 3. It is apparent that there were similar trends of TEMPO oxidation in the ultrasonic system. In the first two hours, the oxidation was fast, and the content of available chlorine dropped quickly. After four hours of oxidation, the consumption of available chlorine was minute.

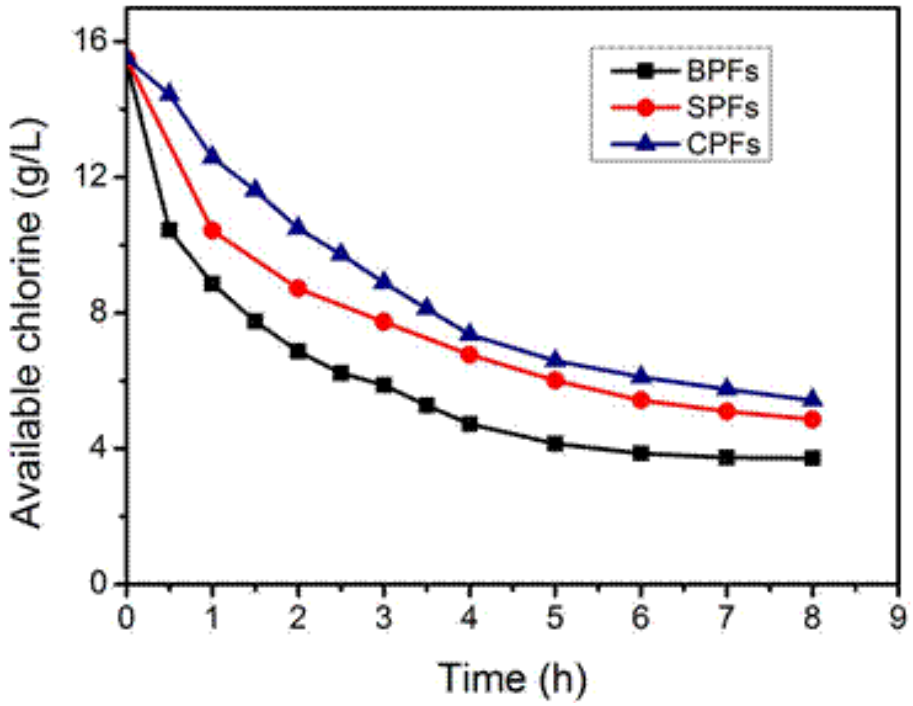

Fig. 3. Residual available chlorine of BPFs, SPFs, and CPFs in the mixtures *vs.* reaction time. (Reaction was carried out by TEMPO-NaBr-NaClO oxidation under the condition of ultrasonic cleaner with working frequency 40 kHz.)

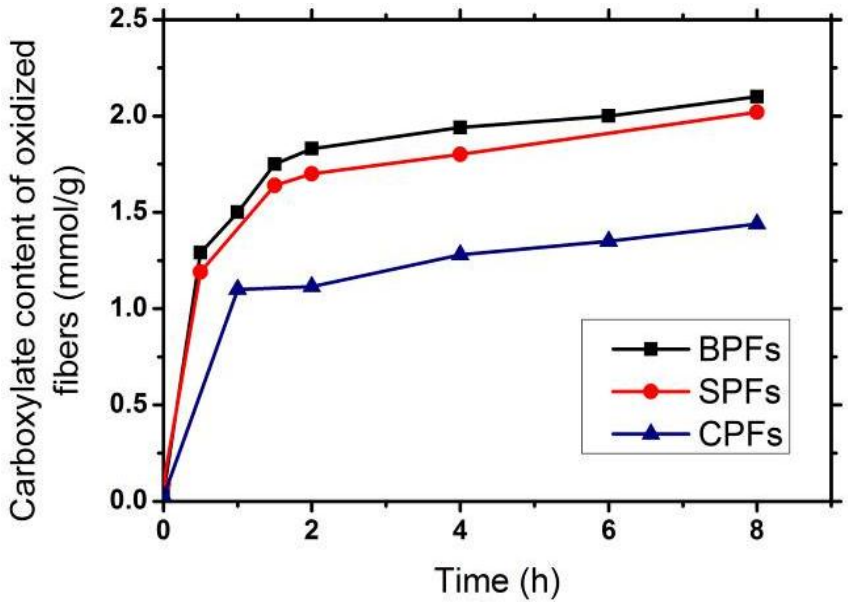

Fig. 4. Carboxylate content of oxidized BPFs, SPFs, and CPFs in the mixtures *vs*. reaction time

However, in Fig. 3, the curve corresponding to CPFs was the highest of all curves, while that of BPFs was the lowest. This indicates that BPFs and CPFs consumed the most and the least sodium hypochlorite, respectively, during the reaction. The difference partly came from the different crystallinities and microstructures of fibers. It was discovered that the crystallinities of BPFs, SPFs, and CPFs were 66.1%, 72.3%, and 83.7%, respectively. BPFs had more amorphous region, and such amorphous material can be oxidized and split out for further oxidation. Moreover, most of CPFs region was crystalline and thus resistant to oxidation. Since the crystallinity of SPFs (72.3%) was between the crystallinity values of BPFs and CPFs, SPFs had a superior reactivity to CPFs but an inferior reactivity to BPFs. Besides, the crystal sizes also affected the oxidation rate, since the oxidation could take place on the surface of crystalline regions. CPFs had the biggest crystal size and the highest crystallinity, so the oxidation could be the most difficult. As explained before, BPFs had the most amorphous regions and small crystal size, and oxidation was easier for BPFs. From the aspect of microstructure, CPFs were much more compact, and the ultrasonication was less effective, so it was hard for reagents to permeate, and thus, the oxidation would be retarded. BPFs and SPFs had relatively loose microstructures, so ultrasonication was efficient, and both the permeation of reagents and oxidation were accelerated. As a result, the curve of CPFs declined in a relatively mild way, and the consumption of available chlorite was much less than that of BPFs and SPFs.

Another reason for the difference was that cotton linter pulp contained pure cellulosic fibers, but both bamboo pulp and softwood pulp contained hemicellulose, which contains side-chains and causes more amorphous region and reaction surface. Besides, bamboo pulp also contained parenchyma cells, which could have consumed available chlorite for its oxidization. Hemicellulose and parenchyma cell content could be another reason causing differences in consumption of available chlorite.

Carboxylate content of oxidized fibers

The carboxyl groups of oxidized fibers were determined by the electrical conductance titration method, and results are shown in Fig. 4. For oxidized BPFs and SPFs, the trends rose quickly in the first two hours, then decreased, and finally plateaued. However, the oxidized CPFs had another increasing trend: the uptrend was obvious in the first hour, but then it went up slowly for the next seven hours. For oxidized BPFs, the ultimate content of carboxyl group was 2.10 mmol/g, and for SPFs it was 2.02 mmol/g, respectively. But for CPFs, after being oxidized by TEMPO mediated oxidation in the ultrasonic system for eight hours, the final carboxyl group content was 1.4 mmol/g. Even when CPFs were oxidized for 14 hours, the ultimate content of carboxyl group was 1.66 mmol/g.

The differences in carboxylate content were consequences of the materials' crystallinities and microstructures. As CPFs had the highest crystallinity, the amorphous region that can be destroyed to increase surface area was limited, so after most of the amorphous region was exposed to reagents and then oxidized in the intensive treatment by ultrasonic generator, little reactivity remained. More energy and time were needed to destroy the residual amorphous region and expose the surface of the crystalline region, which explains why the uptrend seemed slower and milder. The crystallinities for BPFs and SPFs were low, and their surfaces were full of folds and cracks, so responses to both the ultrasonication and oxidation were achieved more easily and faster. The ultimate content of BPFs was the highest, followed by the SPFs, and ending with CPFs, which corresponded to their crystallinities and microstructures.

Appearance and Transmission Electron Microscope (TEM) Images of Cellulose Nanocrystals

From Fig. 5 it is apparent that the BPFs' nanocrystal gels (bottle A) were the most transparent, and softwood nanocrystal gel (bottle B and C) was more turbid. Cotton linter nanocrystal gel (bottle D) was the least transparent.

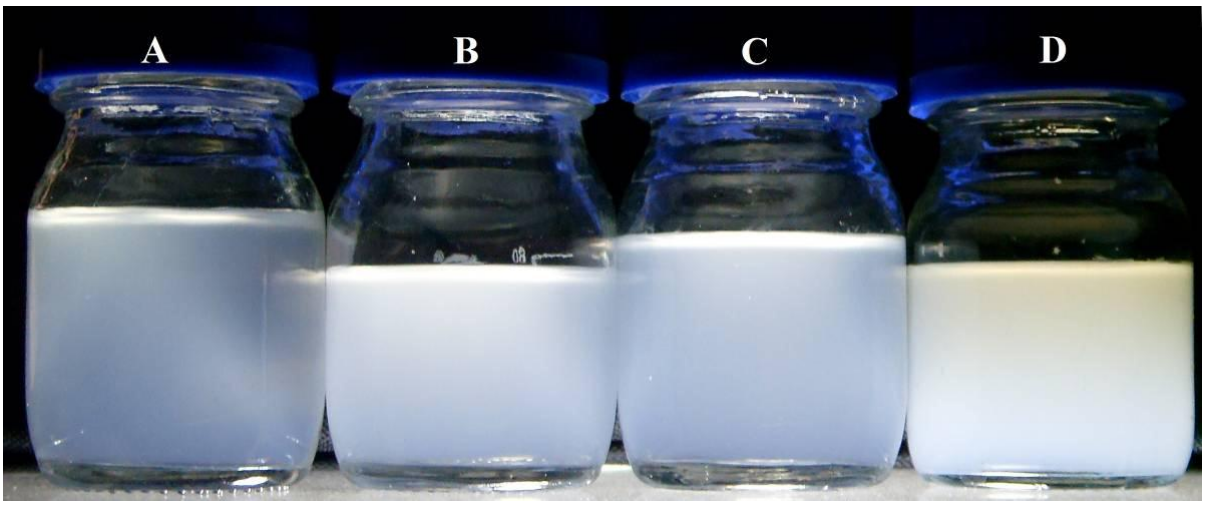

Fig. 5. Appearance images of nanocrystal gels of 1% (pH 2 to 3) after ultrasonic-assisted oxidation: (A) BPFs' nanocrystals after 8 hrs oxidation; (B) SPFs' nanocrystals after 8 hrs oxidation; (C) SPFs' nanocrystals after 10hrs oxidation; (D) CPFs' nanocrystals after 14 hrs oxidation

After eight hours of reaction time, few fine fragments could be found directly by eyes, so extended ultrasonic treatment was applied until fine particles could not be found directly. Comparison of bottle B and C shows that a longer reaction time could render the nanocrystal gel more transparent.

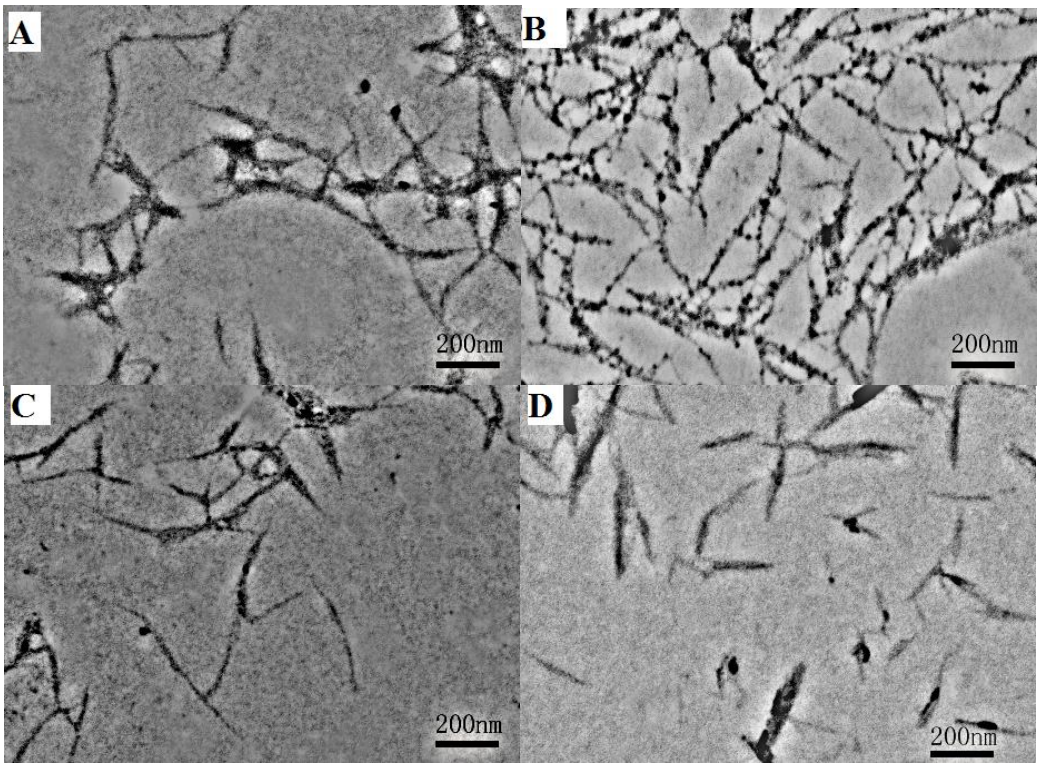

Fig. 6. TEM images: (A) the BPFs' nanocrystals after 8 hrs oxidation; (B) and (C) the SPFs' nanocrystals after 8 hrs and 10 hrs oxidation, respectively; (D) the CPFs' nanocrystals after 14 hrs oxidation with ultrasonic assistance

As shown in Fig. 6, it is justifiable to classify these oxidized products with ultrasonic treatment as nanoscale particles. Images showed that most of the BPFs' nanocrystals were 400 to 800 nm in length and 5 to 15 nm in width, and few reached 1 μm in length, respectively. When oxidized with ultrasonication for 8 hrs, most of SPFs' nanocrystals were 400 to 800 nm in length and 5 to 15 nm in width, respectively. However, when the reaction was extended to ten hours, the length was decreased to 400 to 600 nm, while the width changed little. As shown in Fig. 6(D), the CPFs' nanocrystals were 10 to 25 nm in width and 200 to 400 nm in length, respectively. The length of SPFs' nanocrystals and CPFs' nanocrystals were relatively uniform, while there were many shorter nanocrystals in the BPFs' nanocrystal suspensions. The nanocrystals consist of the residual amorphous and crystalline region after oxidation and ultrasonication. BPFs' nanocrystals were the longest, since there was still relatively much amorphous region in the nanocrystals, which could be found in Table 1. More amorphous region also meant more crystalline region was linked in a nanocrystal because amorphous and crystalline regions were connected in alternating fashion. SPFs' nanocrystals in image (B) were longer than those in image (C), which revealed that longer ultrasonication destroyed more amorphous region. CPFs' nanocrystals were the shortest, because CPFs have the highest crystallinity, the most compact microstructures, and the longest ultrasonic treatment.

CONCLUSIONS

1. Nanocrystals, with high carboxylic acid content, were produced by direct ultrasonic-assisted TEMPO oxidation from BPFs, SPFs, and CPFs. The length of nanocrystals which were produced from BPFs, SPFs, and CPFs were 200 to 800 nm, 200 to 800 nm, and 200 to 400 nm, respectively; the widths were 5 to 15 nm, 5 to 15 nm, and 10 to 25 nm, respectively.
2. The carboxylate content of nanocrystals produced from BPFs, SPFs, and CPFs were 2.10 mmol/g, 2.02 mmol/g, and 1.66 mmol/g, respectively.
3. The oxidation process of BPFs was the fastest, followed by that of SPFs. The oxidation process of CPFs was the slowest, due to the different crystallinities and microstructures of raw materials.
4. Nanocrystals from BPFs, SPFs, and CPFs were stably dispersed in water.

ACKNOWLEDGMENTS

The authors are grateful for the support of "Twelve Five" Nation Science Support Program, Grant No. 2011BAC11B01, PAPD of Jiangsu Higher Education Institutions, and the fund of Jiangsu Provincial Key Lab of Pulp and Paper Science and Technology, Grant No. 2010-09.

REFERENCES CITED

Abe, K., and Yano, H. (2009). "Comparison of the characteristics of cellulose microfibril aggregates of wood, rice straw, and potato tuber," *Cellulose* 16(6), 1017-1023.

Abe, K., and Yano, H. (2010). "Comparison of the characteristics of cellulose microfibril aggregates isolated from fiber and parenchyma cells of Moso bamboo (Phyllostachys pubescens)," *Cellulose* 17(2), 271-277.

Bolio-Lopez, G. I., Valadez-Gonzalez, A., Veleva, L., and Andreeva, A. (2011). "Cellulose whiskers from agro-industrial banana wastes: Isolation and characterization," *Revista Mexicana De Ingenieria Quimica* 10(2), 291-299.

Chen, W., Yu, H., Liu, Y., Chen, P., Zhang, M., and Hai, Y. (2011a). "Individualization of cellulose nanofibers from wood using high-intensity ultrasonication combined with chemical pretreatments," *Carbohydrate Polymers* 83(4), 1804-1811.

Chen, W., Yu, H., Liu, Y., Hai, Y., Zhang, M., and Chen, P. (2011b). "Isolation and characterization of cellulose nanofibers from four plant cellulose fibers using a chemical-ultrasonic process," *Cellulose* 18(2), 433-442.

Cherian, B. M., Leao, A. L., de Souza, S. F., Manzine Costa, L. M., de Olyveira, G. M., Kottaisamy, M., Nagarajan, E. R., and Thomas, S. (2011). "Cellulose nanocomposites with nanofibres isolated from pineapple leaf fibers for medical applications," *Carbohydrate Polymers* 86(4), 1790-1798.

Eichhorn, S. J., Dufresne, A., Aranguren, M., Marcovich, N. E., Capadona, J. R., Rowan, S. J., Weder, C., Thielemans, W., Roman, M., Renneckar, S., Gindl, W., Veigel, S.,

Keckes, J., Yano, H., Abe, K., Nogi, M., Nakagaito, A. N., Mangalam, A., Simonsen, J., Benight, A. S., Bismarck, A., Berglund, L. A., and Peijs, T. (2010). "Review: current international research into cellulose nanofibres and nanocomposites," *Journal of Materials Science* 45(1), 1-33.

Filson, P. B., and Dawson-Andoh, B. E. (2009). "Sono-chemical preparation of cellulose nanocrystals from lignocellulose derived materials," *Bioresource Technology* 100(7), 2259-2264.

Hubbe, M. A., Rojas, O. J., Lucia, L. A., and Sain, M. (2008). "Cellulosic nanocomposites: A review," *BioResources* 3(3), 929-980.

Huber, T., Muessig, J., Curnow, O., Pang, S., Bickerton, S., and Staiger, M. P. (2012). "A critical review of all-cellulose composites," *Journal of Materials Science* 47(3), 1171-1186.

Kaushik, A., and Singh, M. (2011). "Isolation and characterization of cellulose nanofibrils from wheat straw using steam explosion coupled with high shear homogenization," *Carbohydrate Research* 346(1), 76-85.

Kawasaki, H., Takeda, Y., and Arakawa, R. (2007). "Mass spectrometric analysis for high molecular weight synthetic polymers using ultrasonic degradation and the mechanism of degradation," *Analytical Chemistry* 79(11), 4182-4187.

Klemm, D., Heublein, B., Fink, H. P., and Bohn, A. (2005). "Cellulose: Fascinating biopolymer and sustainable raw material," *Angewandte Chemie-International Edition* 44(22), 3358-3393.

Li, Q., and Renneckar, S. (2009). "Molecularly thin nanoparticles from cellulose: isolation of sub-microfibrillar structures," *Cellulose* 16(6), 1025-1032.

Li, Q., and Renneckar, S. (2011). "Supramolecular structure characterization of molecularly thin cellulose I nanoparticles," *Biomacromolecules*, 12(3), 650-659.

Lipp-Symonowicz, B., Sztajnowski, S., and Wojciechowska, D. (2011). "New commercial fibres called 'bamboo fibres' - Their structure and properties," *Fibres & Textiles in Eastern Europe* 19(1), 18-23.

Martins, M. A., Teixeira, E. M., Correa, A. C., Ferreira, M., and Mattoso, L. H. C. (2011). "Extraction and characterization of cellulose whiskers from commercial cotton fibers," *Journal of Materials Science* 46(24), 7858-7864.

Mishra, S. P., Thirree, J., Manent, A.-S., Chabot, B., and Daneault, C. (2011). "Ultrasound-catalyzed TEMPO-mediated oxidation of native cellulose for the production of the nanocellulose: effect of process variables," *BioResources* 6(1), 121-143.

Montanari, S., Rountani, M., Heux, L., and Vignon, M. R. (2005). "Topochemistry of carboxylated cellulose nanocrystals resulting from TEMPO-mediated oxidation," *Macromolecules* 38(5), 1665-1671.

Okita, Y., Saito, T., and Isogai, A. (2010). "Entire surface oxidation of various cellulose microfibrils by TEMPO-mediated oxidation," *Biomacromolecules* 11(6), 1696-1700.

Qin, Z., Qian, Y., Tong, G., Qin, Y. C. F., and Li, Z. (2011a). "The preparation of high carboxylate nano-crystals by TEMPO oxidation in ultrasonic system from full bleached bamboo kraft pulp," *16th International Symposium on Wood, Fiber and Pulping Chemistry*, Tianjin, China, 499-502.

Qin, Z., Tong, G., Chin, Y. C. F., and Zhou, J. (2011b). "Preparation of ultrasonic-assisted high carboxylate content cellulose nanocrystals by TEMPO oxidation," *BioResources* 6(2), 1136-1146.

Ray, A. K., Das, S. K., Mondal, S., and Ramachandrarao, P. (2004). "Microstructural characterization of bamboo," *Journal of Materials Science* 39(3), 1055-1060.

Saito, T., and Isogai, A. (2004). "TEMPO-mediated oxidation of native cellulose. The effect of oxidation conditions on chemical and crystal structures of the water-insoluble fractions," *Biomacromolecules* 5(5), 1983-1989.

Saito, T., Kimura, S., Nishiyama, Y., and Isogai, A. (2007). "Cellulose nanofibers prepared by TEMPO-mediated oxidation of native cellulose," *Biomacromolecules* 8(8), 2485-2491.

Samir, M., Alloin, F., and Dufresne, A. (2005). "Review of recent research into cellulosic whiskers, their properties and their application in nanocomposite field," *Biomacromolecules* 6(2), 612-626.

Shi, S., and He, W. (2010). *Pulping and Making Paper Analysis and Detection*, China Light Industry Press, Beijing. 121-122.

Stelte, W., and Sanadi, A. R. (2009). "Preparation and characterization of cellulose nanofibers from two commercial hardwood and softwood pulps," *Industrial & Engineering Chemistry Research* 48(24), 11211-11219.

Teixeira, E. d. M., Correa, A. C., Manzoli, A., Leite, F. d. L., de Oliveira, C. R., and Capparelli Mattoso, L. H. (2010). "Cellulose nanofibers from white and naturally colored cotton fibers," *Cellulose* 17(3), 595-606.

Wegner, T. H., and Jones, P. E. (2006). "Advancing cellulose-based nanotechnology," *Cellulose* 13(2), 115-118.

Article submitted: April 19, 2012; Peer review completed: July 3, 2012; Revised version received: August 15, 2012; Accepted: August 18, 2012; Published: August 21, 2012.